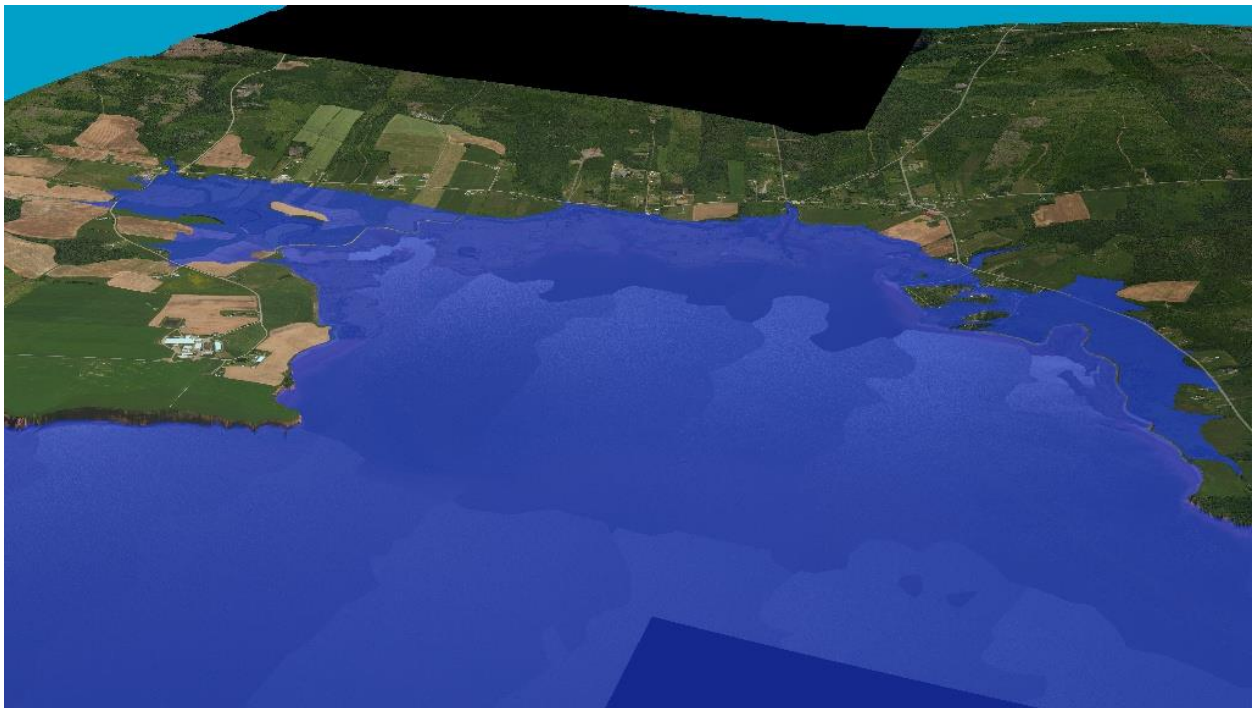


Coastal Vulnerability and Projected Erosion in East Hants County



Nova Scotia Community College
Applied Geomatics Research Group
NSCC, Middleton, NS
Tel. 902 825 5475
Email: timothy.webster@nsc.ca

Rachel Gilbert, MCIP LPP
Manager of Planning
Municipality of East Hants
15 Commerce Court Elmsdale, NS B2S 3K5
February 14, 2022

Coastal Vulnerability and Projected Erosion in East Hants County

How to cite this work and report:

NSCC Applied Geomatics Research Group. 2022. Coastal Vulnerability and Projected Erosion in East Hants County. Technical report, Applied Geomatics Research Group, NSCC Middleton, NS.

Copyright and Acknowledgement

The Applied Geomatics Research Group of the Nova Scotia Community College maintains full ownership of all data collected by equipment owned by NSCC and agrees to provide the end user who commissions the data collection a license to use the data for the purpose they were collected for upon written consent by AGRG-NSCC. The end user may make unlimited copies of the data for internal use; derive products from the data, release graphics and hardcopy with the copyright acknowledgement of **“Data acquired and processed by the Applied Geomatics Research Group, NSCC”**. Data acquired using this technology and the intellectual property (IP) associated with processing these data are owned by AGRG/NSCC and data will not be shared without permission of AGRG/NSCC.

Table of Contents

- 1. Introduction 1
- 2. Methods 6
 - 2.1. Coastal Erosion Metrics 6
 - Coastal Flooding 8
 - 2.2. 8
- 3. Results 9
 - 3.1. Coastal Erosion 9
 - 3.2. Flood Risk 14
- 4. Discussion 18
- 5. Conclusions 26
- 6. References 28

Table of Figures

Figure 1. East Hants coastal erosion and flood analysis area of interest.	6
Figure 2. Digitized coastlines from the Shubenacadie River to Noel Shore, NS.	9
Figure 3. Digitized coastlines for the Noel Shore to Moose Brook, NS.....	9
Figure 4. Digitized coastlines from Moose Brook to Walton, NS.....	10
Figure 5. Classified erosion rates over the entire coastline showing a greater risk to the east of Sloop Rocks versus the western region.	10
Figure 6. Classified erosion rates from the Shubenacadie River to Noel Shore, NS.	11
Figure 7. Classified erosion rates for the Noel Shore to Moose Brook, NS.	11
Figure 8. Classified erosion rates from Moose Brook to Walton, NS.	12
Figure 9. Comparison of 5 coastlines.....	12
Figure 10. Historical coastlines and how future erosion could impact coastal residential areas without armoring.....	13
Figure 11. Present day flood risk level between Shubenacadie River and Noel Shore.	14
Figure 12. Present day flood risk between Noel Shore and Moose Brook.	14
Figure 13. Present day flood risk between Moose Brook and Walton.....	15
Figure 14. 100-year flood risk between Shubenacadie and Noel Shore.....	15
Figure 15. 100-year flood risk between Noel Shore and Moose Brook.....	16
Figure 16. 100-year flood risk between Moose Brook and Walton.....	16
Figure 17. An example of properties that could be directly affected by the present-day flood risk.	17
Figure 18. Comparison of orthophotos and coastlines. A) 1973 orthophoto map and coastline (yellow). B) 2002 orthophoto image and coastline (cyan). C) 2013 orthophoto image and coastline (magenta). D) 2019 lidar DEM colour shaded relief image and coastline (grey).	19
Figure 19. Comparison of coastline positions from historical imagery/lidar. A) Coastlines derived from 2002 (cyan) and 2013 (magenta). B) Coastlines derived from 1973 (yellow), 2013 (magenta) and 2019 lidar DEM (grey).	20
Figure 20. Comparison of LT and ST erosion rates. A) Erosion rate LT statistics between the 1973 and 2019 coastlines. Average rate of 83 cm/year with a standard deviation of 76 cm/year. B) Erosion rate ST statistics between the 2013 and 2019 coastlines. Average rate of 190 cm/year with a standard deviation of 225 cm/year.....	21
Figure 21. Trees that obscure the 2013 coastline are removed in the 2019 lidar.....	23
Figure 22. Modified coastlines where the 1973 tidal flat has been omitted.....	24
Figure 23. Digitized coastlines along a waterway in 1973 and a salt marsh in 2013.....	25
Figure 20. Major flooding in the Noel area under 100-year flood conditions.....	26
Figure 21. Dykes near Burntcoat (top) and Noel Shore (bottom) under present day flood risk conditions.	27

List of Tables

Table 1. Classified erosion rates for East Hants.....	7
Table 2. Flood risk parameters for Hants County, NS.....	8

1. Introduction

Approximately 10% of the world's population live only 10 m above the current sea level, putting this population at risk of flooding. Observations of the global mean sea level (GMSL) show it is rising and the rate has been accelerating since 2000 (Golledge, 2020). The increased rate of sea level rise has largely been attributed to increased ocean warming (Cheng *et al.*, 2019), which can be linked to global warming.

James *et al.* (2014) reported on global sea-level rise (SLR) based on the latest IPCC AR5 report (Church *et al.*, 2013). In the AR5 report, Representative Concentration Pathway (RCP) scenarios were used to generate SLR projections considering CO₂ estimates. The SLR projections in AR5 include contributions from the thermal expansion of the ocean (steric effect), land ice melting and discharge, and anthropogenic influences. The AR5 global sea-level rise projections from Church *et al.* (2013) state a mean value of 0.74 m [0.52 m to 0.98 m] and the footnote states "Bracketed values represent the 5% and 95% confidence intervals about the mean value". James *et al.* (2014) report the same values for the RCP8.5 global sea-level projection for 2100 but the footnote states, "Numbers are the median value and the 5% and 95% confidence range of sea-level rise relative to 1986-2005". It is interesting to note that there appears to be a discrepancy in the James *et al.* (2014) abstract where they state, "The global mean sea-level projection for RCP8.5, the largest emissions scenario, at 2100 is 74 cm (5%-95% range is 54 to 98 cm)." James *et al.* (2014) Table C7 Projected Relative Sea-level Change at 2010 and 2100 for RCP8.5.

The Canadian Extreme Water Level Adaptation Tool (CAN-EWLAT) produced by DFO did a similar study to James *et al.* (2014) where they used the IPCC AR5 projection and GPS data for Glacial Isostatics Adjustment (GIA) for all the Small Craft Harbours in the country (<http://www.bio.gc.ca/science/data-donnees/can-ewlat/index3-en.php>). They utilized the tide gauge records to calculate the return periods of total water level (Zhai *et al.*, 2015) and where tide gauges were not available, they used the storm surge model methods similar to Bernier and Thompson (2006).

The DFO work by Han *et al.* (2016) developed regional mean SLR scenarios for Canada: "Low", "Intermediate", and "High", based on three global mean SLR scenarios. Based on the IPCC AR5 assessment (Church *et al.*, 2013), they first modified the four global mean sea level rise scenarios over 1992-2100 used in the United States (Parris *et al.*, 2012). For the "Low Scenario", the regional SLR values were projected using past linear trends estimated from tide-gauge data at individual stations. For the "Intermediate Scenario", they used the sea level projections from IPCC AR4 A2 and AR5 RCP8.5 emission scenarios. Their "High Scenario" is the same as the US Intermediate-High Scenario (1.2 m). They did not consider the US "Highest Scenario" of 2.0 m (Parris *et al.*, 2012), because this scenario is of low confidence according to the IPCC AR5 assessment (Church *et al.*, 2013). The global scenarios were adjusted for three factors that affect local mean sea levels. The first factor is the net effect of the glacial isostatic adjustment from a model, with its vertical land motion further replaced by satellite Global Positioning System (GPS) data. The second is the steric and dynamic ocean effect obtained from the ensemble of global climate models. The third is the model-based land-ice melt effect.

The NOAA (2017) report presented linkages between scenarios based on probabilistic projections for future sea level rise for coastal-risk planning, management of long-lived critical infrastructure, mission readiness, and other purposes. The projections and results presented in several peer-reviewed publications provide evidence to support a physically plausible Global Mean Sea Level (GMSL) rise in the

range of 2.0 meters (m) to 2.7 m, and recent results regarding Antarctic ice-sheet instability indicate that such outcomes may be more likely than previously thought. To ensure consistency with these recent updates to the peer-reviewed scientific literature, they recommend a revised 'extreme' upper-bound scenario for GMSL rise of 2.5 m by the year 2100, which is 0.5 m higher than the upper bound scenario from Parris *et al.* (2012).

Parris *et al.* (2012) recommended a scenario approach covering a broad range (0.2 m to 2.0 m GMSL rise by 2100) of existing sea level study results (trends, process modeling, semi-empirical approaches, etc.). Parris *et al.* (2012) explicitly conceptualized scenarios as being defined by considerations of use, writing, "Scenarios do not predict future changes, but describe future potential conditions in a manner that supports decision-making under conditions of uncertainty. Scenarios are used to develop and test decisions under a variety of plausible futures. This approach strengthens an organization's ability to recognize, adapt to, and take advantage of changes over time".

In the NOAA (2017) report they indicate that an assessment of recent probabilistic studies finds GMSL rise by 2100 projected for the 90% probability (5th–95th% confidence interval) range to fall between 0.5–1.3 m, for RCP8.5 (Miller *et al.*, 2013; Kopp *et al.*, 2014, 2016a; Slangen *et al.*, 2014; Mengel *et al.*, 2016).

Since the upper limit established by Pfeffer *et al.* (2008), which was based primarily on an assessment of the maximum plausible loss rate from Greenland and which was the basis for the 2.0 m high scenario for 2100 of Parris *et al.* (2012), there has been continued and growing evidence that both Antarctica and Greenland are losing mass at an accelerated rate based upon gravimetry satellites (GRACE), repeat altimetry, in-situ GPS monitoring, and input-output calculations (Shepherd *et al.*, 2012; Khan *et al.*, 2014; Scambos and Shuman, 2016; Seo *et al.*, 2015; Martín-Español *et al.*, 2016). Such evidence suggests that the collapse of some sectors of the Antarctic ice sheet may be inevitable as surrounding ocean waters warm (Joughin *et al.*, 2014; Rignot *et al.*, 2014). Kopp *et al.* (2014) discuss several lines of arguments that support a plausible worst-case GMSL rise scenario in the range of 2.0 m to 2.7 m by 2100. Thus, to ensure consistency with the growing number of studies supporting upper GMSL bounds exceeding Pfeffer *et al.* (2008)'s estimate of 2.0 m by 2100 and the potential for continued acceleration of mass loss and associated additional rise contributions now being modeled for Antarctica, this report recommends a revised worst-case (Extreme) GMSL rise scenario of 2.5 m by 2100.

The NOAA (2017) report also described similar methods that were applied by James *et al.* (2014), Zhai *et al.* (2015), and Han *et al.* (2016). Regional relative sea level rise (RSLR) projections or scenarios that account for static-equilibrium fingerprints, oceanographic processes, and vertical land motion (VLM) have been considered in several recent studies (Mitrovica *et al.*, 2011; Yin, 2012; Perrette *et al.*, 2013; Church *et al.*, 2013a; Kopp *et al.*, 2014, 2016a; Horton *et al.* 2015; Slangen *et al.*, 2014; Grinstead *et al.*, 2015; Hall *et al.*, 2016). Results of the regionalization process are shown in section 5 of the NOAA report.

The NOAA (2017) report includes some of the same insights observed by James *et al.* (2014), Zhai *et al.* (2015), and Han *et al.* (2016) stating that future RSLR is amplified along the Northeast U.S. coast because of GIA, the far-field static equilibrium effects of Antarctic melt, and reduced transport of the larger Gulf Stream System, Atlantic Meridional Overturning Circulation (AMOC). Future RSLR is partially reduced by intermediate-field static-equilibrium effects associated with relative proximity to Greenland and many northern glaciers. They summarized their report by stating that they have provided results and discussion related to two primary tasks: 1) developing an updated scenario range for possible 21st

century GMSL rise and 2) producing a set of gridded RSLR response along the United States coastline based on discrete scenarios drawn from this updated GMSL rise range. From this revised range for GMSL rise, RSLR is projected on a 1-degree grid (and for precise locations of tide gauges) covering the U.S. mainland coastline, Alaska, Hawaii, the Caribbean, and the Pacific island territories for six representative GMSL rise scenarios by 2100: a “Low”, “Intermediate-Low”, “Intermediate”, “Intermediate-High”, “High”, and “Extreme”, which correspond to GMSL rise of 0.3 m, 0.5 m, 1.0 m, 1.5 m, 2.0 m and 2.5 m, respectively. They conclude that for almost all future GMSL rise scenarios, RSLR is projected to be greater than the global average along the coasts of the U.S. Northeast and the western Gulf of Mexico.

The NOAA (2017) also examined how the projections would impact their tidal flood frequencies. The elevation threshold used to classify such minor (nuisance) flooding events by NOAA based on their tide gauges varies along the U.S. coastline, but in general it is about 0.8 m above the highest average tide and locally has a 20% annual chance of occurrence. Using this flood-frequency definition, we find at most locations examined (90 cities along the U.S. coastline outside of Alaska) that with only about 0.35 m of local RSLR, annual frequencies of such disruptive/damaging flooding will increase 25-fold by or about (± 5 years) 2080, 2060, 2040 and 2030 under the “Low”, “Intermediate-Low”, “Intermediate”, and “Intermediate High” subset of scenarios, respectively.

The NOAA (2017) report concludes by stating that the next steps will focus on the integration of these global and regional scenario products within the diversity of coastal risk management tools and capabilities deployed by individual agencies in support of the needs of specific stakeholder groups and user communities. This deployment of scenarios and tools will help serve as a starting point for on-the-ground coastal preparedness planning and risk management processes needed to ensure that U.S. coastal communities (and their economies) remain vibrant and resilient to ongoing and future changes in sea level.

Daigle (2017) adequately describes the phenomenon of GSL and the regional effects of finger printing, GIA, and dynamic ocean currents. Daigle (2017) Table 3 shows the decadal global SLR values from AR5 and appears correct. Daigle (2017) Table 5 shows the total regional sea-level rise including the potential increased tidal range effect in the Bay of Fundy of 10 cm by 2100 and indicated the 95% confidence interval for the 2100 projections originated from James *et al.* (2014) at + 38 cm and the uncertainties for 2050 and 2030 were scaled using the IPCC rate of increase in Table 3.

The Daigle (2017) report uses the HHWLT limit as a starting point to project storm surge water levels occurring today and into the future with RSLR. This is a reasonable place to start, however Daigle (2017) does point out that the HHWLT values are only available at select tidal stations from the Canadian Hydrographic Service. Daigle translated these tidal datums from their original Chart Datum value (typically based on the lowest astronomical tidal level) to the Canadian Geodetic Vertical Datum of 1928, CGVD28. Many jurisdictions in Canada are adopting the new CGVD2013 vertical datum, as is the vertical reference for the GeoNova Lidar datasets. The CGVD2013 is a better fit representing the geoid across the entire country although it does not relate to mean sea level as closely as CGVD28 did. For example, Halifax is 60 cm below the CGVD2013 datum, and this will undoubtedly cause confusion to non-geomatics professionals working along the coastal zone when it is adopted. The Canadian Hydrographic Service, DFO has release their continuous vertical data reference surfaces which presents the relationship of HHWLT to CGVD2013 for points along the coast spaced at 100 m. Daigle (2011, 2012, 2014) all use the Bernier (2005) thesis to calculate the return period of storm surge water levels. Bernier

(2015) calculated the storm surge return period values by subtracting the total observed water level from the predicted tide level for tide gauge location in Atlantic Canada. These residual or surge values were then used in the extreme analysis to calculate return period and probabilities of occurrence. In previous reports by Richards and Daigle (2011) "Scenarios and Guidance for Adaptation to Climate Change and Sea-Level Rise – Nova Scotia and Prince Edward Island Municipalities" limitations of the methods used by Bernier were made clear to the reader. For example, *"It should be noted that the above-mentioned Total Sea Levels do not include the possibility of an extremely rare historical event such as the Saxby Gale (1869), the Groundhog Day Storm (1976) or of a direct hit by a hurricane (i.e. Hurricane Juan 2003). From a precautionary principle approach to risk management it is advisable to consider the impacts of a plausible upper bound water level that would combine the upper limits of global sea-level rise, local crustal subsidence and the highest storm-surge factor previously recorded by a tide gauge, or where available, some high precision measurements of identified high water marks."*

Webster *et al.* (2012) reported on flood risk for five coastal communities in NS including Minas Basin. Webster *et al.* (2012) used a RSLR value of 73 cm and 146 cm per century for their climate change sea level rise projections. In addition to generating flood risk maps from lidar derived DEMs, they also analyzed tide gauge records of total water level to estimate return periods of extreme water levels. The closest tide gauge in the Bay of Fundy is Saint John, NB. However, they point out that the tidal range is significantly different in Saint John than it is in the Minas Basin. By examining the tide gauge records for Saint John, the Groundhog Day storm of Feb. 2, 1976, shows up as one of the highest water levels recorded at a value of 9.14 m above local chart datum (CD). This water level was observed again in Jan. 1997. The extreme value analysis showed that under current sea level rise conditions, calculated to be 22 cm/century based on the tide gauge records, this value is expected to occur at least once every 33 years from 2010. This return period decreases to occur at least once every 22 years with a RSLR of 0.73 m/century and decreases to occur at least once every 16 years with a RSLR of 1.46 m/century. The 100-year return period water level is 9.24 m CD, which is close to the Groundhog Day storm. With increased RSLR of 0.73 m/century the 100-year water level increases to 9.63 m CD and with RSLR of 1.46 m/century further increases to 10.28 m CD.

Van Proosdij *et al.* (2018) was commissioned by NS Department of Agriculture to conduct a study of dyke vulnerability to SLR and climate change. They used a combination of predicted Higher High Water Large Tide (HHWLT) plus SLR plus the 100-year return period storm surge prediction to produce flood maps for the dyked areas. For dykes in Kings and Hants County they rely on the sea level rise predictions from Daigle (2016). It should be noted that they used the older CDVD28 vertical datum for their estimates, while this study uses the new CGVD2013. There is a difference of approximately 65 cm between these two vertical datums. Daigle (2016) calculated the 100-year storm surge return period, based on Bernier (2005) work, for Saint John, NB to be 1.13 m +/-0.2 m.

Van Proosdij and Jahncke (2019) produced another report with guidelines for sea level rise and storm surge projections. They present very similar information as the 2018 report and used the same recommendation for predicting water levels for coastal flooding (HHWLT + RSLR + Storm Surge) and recommend adding an additional 65 cm to account for the possible collapse of the western Arctic ice sheet.

Coastal Vulnerability and Projected Erosion in East Hants County

The Nova Scotia Community College – Applied Geomatics Research Group (NSCC-AGRG) has been contracted to produce coastal flood maps depicting flood extents for present day and 2100 flood levels based on the cited literature.

Coastal erosion is affected by several factors, one of which is wave climate (BIO, 2021). Ocean waves are affected by winds, and the largest waves are often a result of marine storms, which can produce the largest winds. While North Atlantic storms are expected to face minimal change in the next 50 years, warming temperatures due to climate change could have a significant effect on sea ice (FitzGerald & Hughes 2019). A reduction of sea ice could have a double effect on coastlines, through increasing sea level and allowing for a greater fetch area for winds, which could increase wave size.

The province of Nova Scotia (NS) has 241 km of dykes along its coasts and waterways which protect 16,139 Ha of agricultural marshland from sea level rise and flooding (van Proosdij et al. 2018). Approximately 70% of dyke tracts in NS were calculated to be at “High” or “Very High” risk of coastal erosion and overtopping by 2050. Dr. van Proosdij calculated a foreshore change rate of -0.21 ± 3.06 m for Colchester and concluded that the marshes in Noel Shore and Burntcoat were highly vulnerable to dyke overtopping. These dykes are predicted to be overtopped in approximately 20 years. Dykes in Colchester were approximately twice as likely to overtop at the projected 2100 sea level rise condition versus the 2050 sea level rise conditions (van Proosdij et al. 2018). By 2100, sea levels are predicted to increase over 0.90 m along the Atlantic coast (James et al. 2014).

NSCC-AGRG has been contracted to produce estimates on the rate of coastal erosion through the analysis of historical coastline positions captured in aerial photography and lidar elevation models. Coastlines, defined as the top of the slope, were used rather than shoreline, mean high-water level, to measure erosion between data collections.

2. Methods

Coastal erosion and flooding analysis was focused on a 79 km of coastline within East Hants between Walton and Maitland (Figure 1). This area of interest (AOI) is known to be prone to flooding and rapid coastal erosion. The following sections detail the methods of quantifying these processes.



Figure 1. East Hants coastal erosion and flood analysis area of interest.

2.1. Coastal Erosion Metrics

Historical coastline positions were generated from georeferenced aerial photos of the entire study area acquired from the Nova Scotia Geomatics Centre for the years 2013 and 1973. Lidar was used in place of imagery for the most recent coastal position, 2019, as recent imagery was not available.

Coastlines were manually digitized in ArcGIS Pro for each of the captured dates. Where bare earth was visible in the photos, the ledge of the land was used as the coastline. Where vegetation obscured the bare earth, the coastline was drawn near the base or through the middle of the most seaward vegetation, depending on the angle of the photo. Major waterways connected to the ocean were included in the coastline to account for riverine coastal erosion.

Changes in coastline position between dates were calculated using a script developed by NSCC-AGRG. The better-known, Digital Shoreline Analysis System (DSAS) Version 5, created by the United States Geological Survey (USGS), uses a similar logic to compute distances between coastlines. The DSAS uses a cross-sectional approach to computing distances between coastlines while the NSCC-AGRG script uses a nearest Euclidean distance approach. NSCC-AGRG has found that a Euclidian approach is more appropriate for coastlines that are non-linear with channels and outcrops.

Erosion distances were calculated by measuring the nearest distance from the most recent “Reference” coastline (2019) to the “Compared” historical position (2013, and 1973). Coastlines were subdivided into

Coastal Vulnerability and Projected Erosion in East Hants County

1.0 m sections for this comparison to ensure that distances were calculated for each metre of coastline in the AOI. Erosion rates were then computed by dividing the distance by the number of years between surveys to produce an average rate of erosion over the comparison period. Erosion rates were classified into 6 classes to aid with interpretation (Table 1).

Table 1. Classified erosion rates for East Hants.

Class	Erosion Rate (m/year)
0	Accretion (no erosion)
1	0.0 to 0.5
2	0.5 to 1.0
3	1.0 to 1.5
4	1.5 to 2.0
5	Greater than 2.0

Average erosion rates were used to generate estimates on future coastline positions for 2050 and 2100 by multiplying the value calculated for 2019 by 31 and 81 years respectively. The estimated distances were used to buffer the 2019 coastline position to produce the 2050 and 2100 projected coastlines. Comparative analysis between the long-term (1973-2019) and short-term (2013-2019) erosion estimations demonstrated more consistency along the coast in the long-term scenario and very high variability in the short-term scenario. It was decided that long-term rates were more applicable for predicting future coastline positions.

2.2. Coastal Flooding

Based on the previous studies and the latest literature on SLR we have used the following methods to complete the flood level calculations relative to CGVD2013. Present day and year 2100 flood risks were calculated using an equation from Jamieson *et al.* 2019:

$$\text{Total Sea Level (m)} = \left[\begin{array}{l} \text{Higher High Water Large Tide (HHWLT) (m)} \\ + \text{Relative Sea Level Rise (climate change + subsidence) (m)} \\ + \text{storm surge (1:20 and 1:100 year values) (m)} \end{array} \right]$$

Values for the equation were taken from van Proosdij *et al.* 2018 (Table 2).

Table 2. Flood risk parameters for Hants County, NS.

Condition	HHWLT (CGVD2013)	100 Year Storm Surge	SLR 2100	Ice Sheet Melt	Total Level (CGVD2013)
Present Day	7.31 m	1.13 m			8.44 m
2100	7.31 m	1.13 m	0.9 m	0.65 m	9.99 m

Present day flood risk (HHWLT + 100-year storm surge) was calculated to be 8.44 m CGVD2013. For the 100-year flood risk, an additional 0.65 m was added to the calculation to account for a partial collapse of the West Antarctic Ice Sheet (James *et al.* 2014). The 2100 flood risk was calculated to be 9.99 m CGVD2013.

Flood inundation maps were generated in the ArcGIS environment using a script developed by the NSCC-AGRG. The script generated a series of flood levels from lower to an upper elevation limit relative to CGVD2013 at 0.1 m increments. A “still water” flooding method was used which assumed the ocean was a flat plane and did not take wave run-up or the travel time water takes to cross a land surface into account. This method has been proven suitable for generating static flood inundation maps that predict the extend of flooding from the total sea level including tide and surge for planning purposes (Webster *et al.* 2008). Elevation model cells were considered flooded if they were at a lower elevation than the flood layer increment and connected to the ocean. The connectivity logic ensured that no cells remained “dry” despite being lower than the flood elevation if there was a barrier between the ocean and the cell. For example, land behind dyke structures remains dry (unconnected) until the dyke is overtopped despite being much lower than the flood level. The connectivity logic required that a DEM be hydraulically conditioned to ensure that flow pathways were represented in the elevation data. Features such as coastal roadways would act like dykes unless culvert bottom elevations were present in the elevation model to connect two otherwise separate low-lying areas. Hydraulic conditioning was accomplished using a script developed by NSCC-AGRG that leveraged existing Nova Scotia Topographic Database GIS layers to identify and extract elevations for features such as culverts and bridges. Further quality assurance was performed to identify and add any features missing from the database. The DEM was then flooded in 10 cm increments to 15m elevation. The 8.4 m and 10.0 m flood layers were used for the present-day flood risk and 2100 flood risk in the model.

3. Results

3.1. Coastal Erosion

Coastlines were successfully digitized from the Shubenacadie River to the Walton River, NS for the three survey years (1973, 2013 and 2019) (Figure 2 - Figure 4).



Figure 2. Digitized coastlines from the Shubenacadie River to Noel Shore, NS.



Figure 3. Digitized coastlines for the Noel Shore to Moose Brook, NS.

Coastal Vulnerability and Projected Erosion in East Hants County

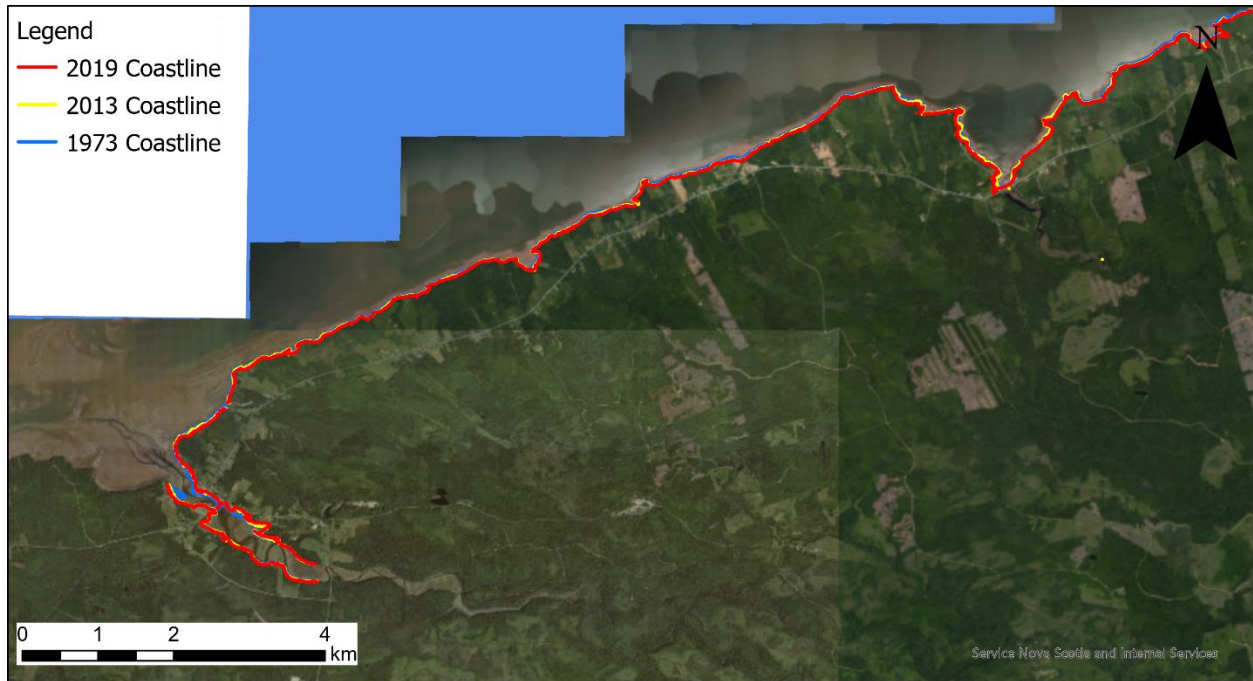


Figure 4. Digitized coastlines from Moose Brook to Walton, NS.

Coastal erosion measurements were successfully computed using the NSCC-AGRGR coastal erosion measurement tool. Classified rates of erosion demonstrated a trend of higher erosion in the eastern extent of the AOI (east of Sloop Rocks) at an average rate of 1.19 m/year with a standard deviation of 0.93 m compared to the western extent at an average rate of 0.48 m/year with a standard deviation of 0.27 m (Figure 5 to Figure 8).

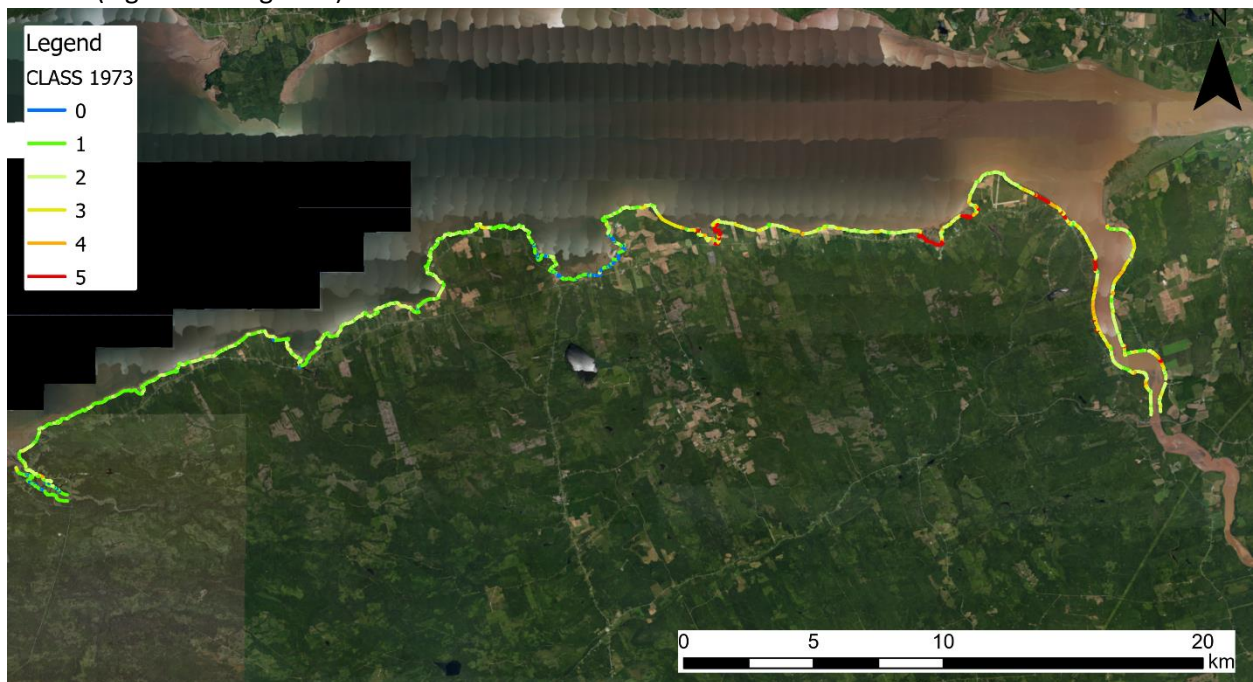


Figure 5. Classified erosion rates over the entire coastline showing a greater risk to the east of Sloop Rocks versus the western region.

Coastal Vulnerability and Projected Erosion in East Hants County



Figure 6. Classified erosion rates from the Shubenacadie River to Noel Shore, NS.



Figure 7. Classified erosion rates for the Noel Shore to Moose Brook, NS.



Figure 10. Historical coastlines and how future erosion could impact coastal residential areas without armoring.

3.2. Flood Risk

Flood modelling was found to produce accurate static water flood maps for connected areas and demonstrated that farmland and infrastructure in dyked areas is prone to flooding for present day flood events of 8.4 m (Figure 11 to Figure 13). The frequency and extent of impact was intensified for future 2100 flood level of 10.0 m (Figure 14 to Figure 16).



Figure 11. Present day flood risk level between Shubenacadie River and Noel Shore.

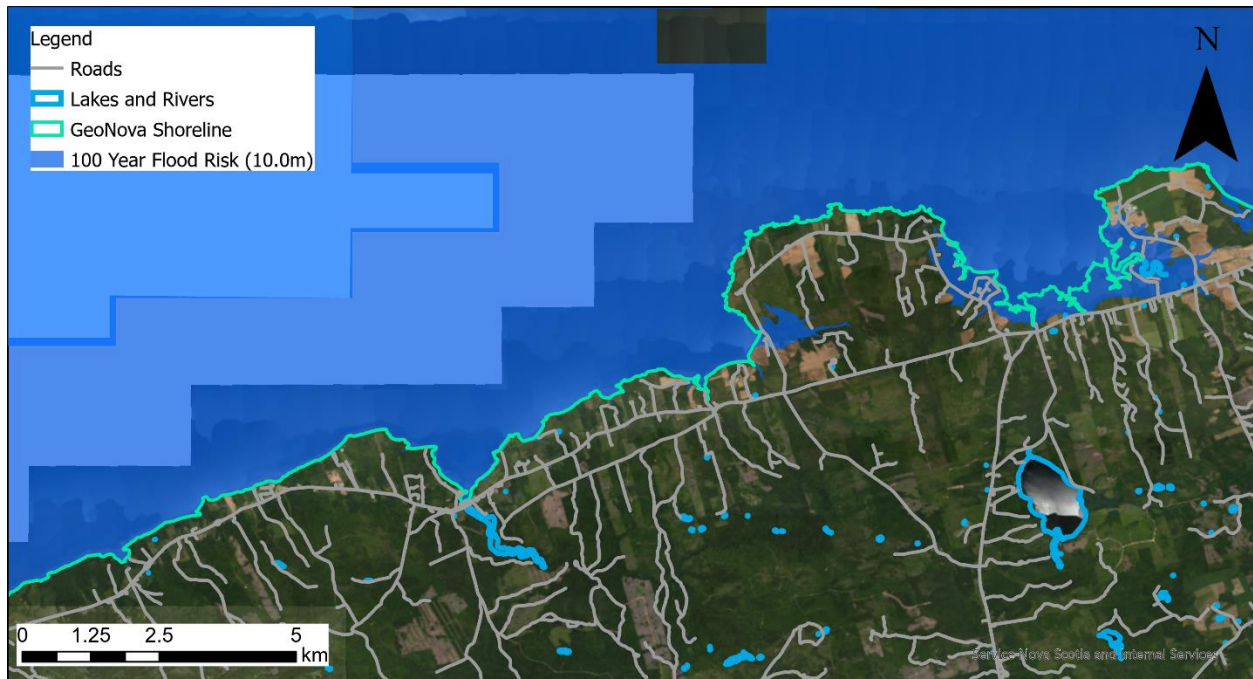


Figure 12. Present day flood risk between Noel Shore and Moose Brook.

Coastal Vulnerability and Projected Erosion in East Hants County

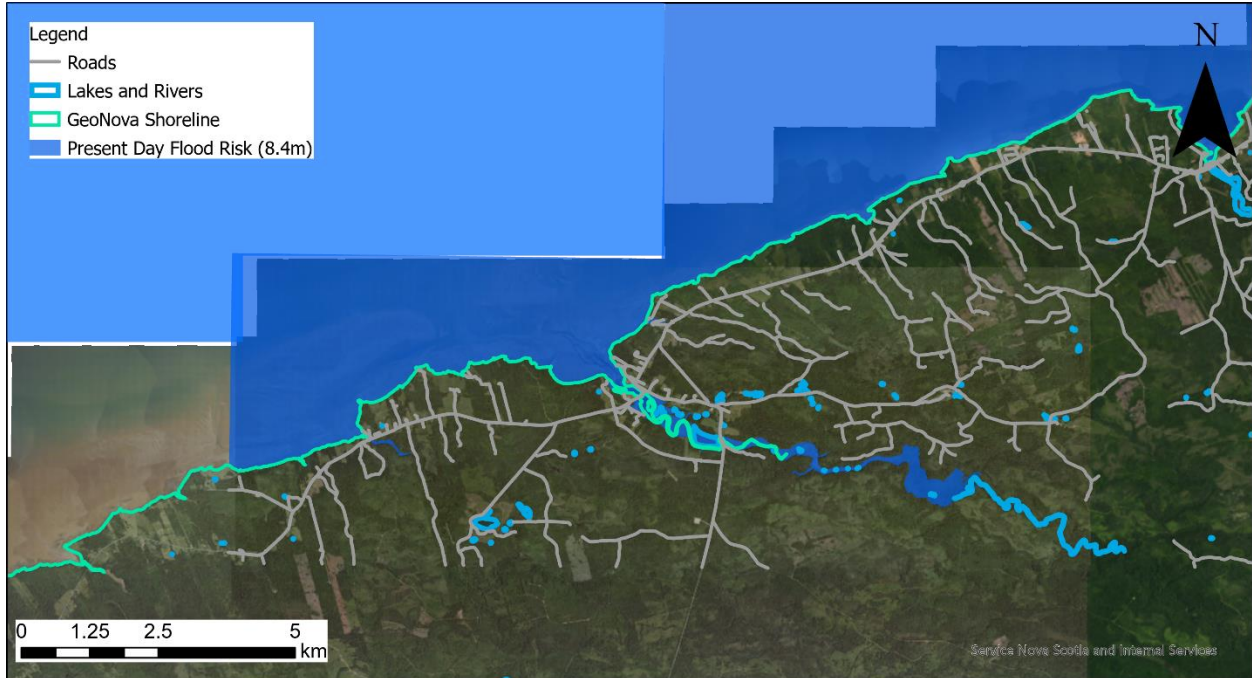


Figure 13. Present day flood risk between Moose Brook and Walton.



Figure 14. 100-year flood risk between Shubenacadie and Noel Shore.

Coastal Vulnerability and Projected Erosion in East Hants County

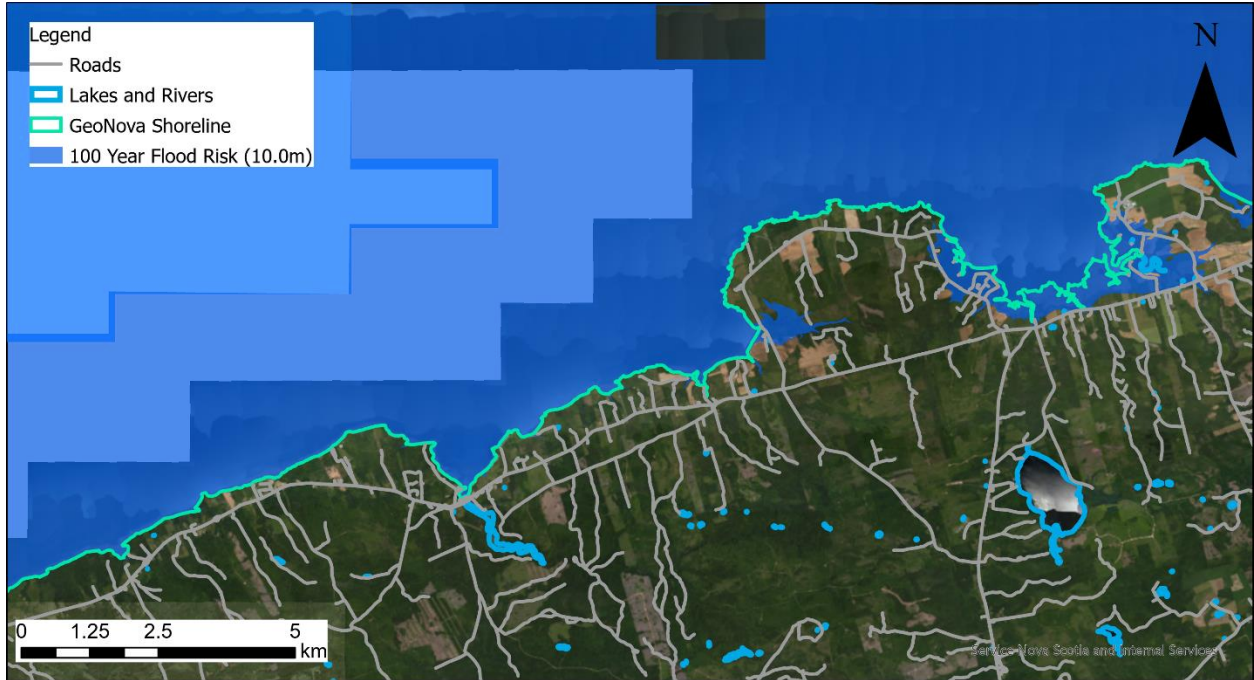


Figure 15. 100-year flood risk between Noel Shore and Moose Brook.

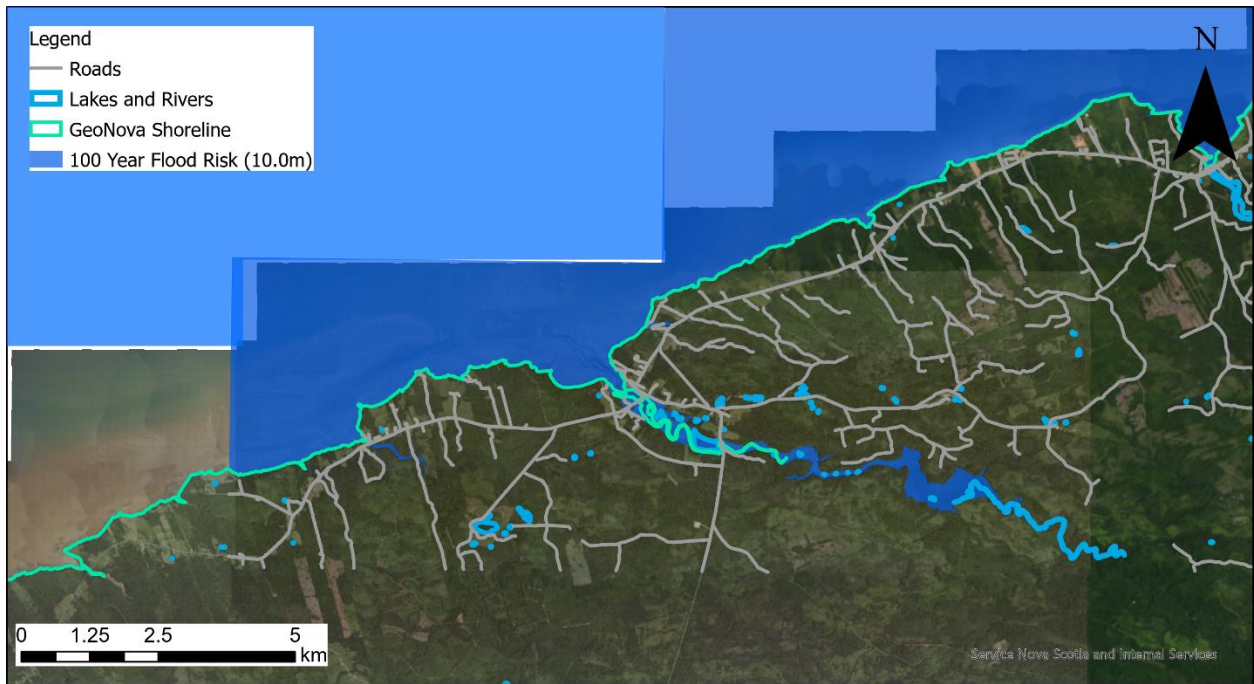


Figure 16. 100-year flood risk between Moose Brook and Walton.

4. Discussion

The calculation of past erosion rates was accomplished by comparing the coastlines interpreted from orthophotos of different dates. Once orthophotos were constructed, the coastline was interpreted for each date of imagery. In this study, the term coastline referred to the geomorphic effect of the ocean on the land, which was distinct from the shoreline, which is defined by GeoNova to represent the mean high-water line. Here, we interpret the coastline to be the top of an eroding bank.

The initial plan was to acquire historic aerial photos of the East Hants coastal zone and orthorectify them. This can be challenging to find accurate and representative ground control points to use to georeference or orthorectify the historical imagery. An orthophoto also has relief displacement removed by utilizing a DEM. To remove the bias of using a present-day DEM, derived from lidar, to orthorectify historical imagery, we attempted to use Structure from Motion techniques to construct a DEM from the historical imagery itself to compensate for relief displacement more accurately. Unfortunately, the historical aerial photos did not have enough overlap to resolve the elevation and obtain a DEM from the historical images. As a result, existing historical orthophotos were used from GeoNova by contacting the NS geomatics Center in Amherst. There were two types of orthophoto products available from GeoNova: orthophoto imagery and orthophoto maps that were on mylar which consisted of the imagery and linework (contours, shoreline, etc.). Scanned orthophoto maps were obtained for 1973 and the orthophoto imagery was obtained for 2002 and 2013. Coastlines were interpreted and digitized from each of these datasets (Figure 18).

Another key point was that the erosion calculations were focused on coastal areas and not inland estuaries except for the Walton River area where part of the estuary was included. The bank of the estuary was clear in the 2019 lidar data but not in the older orthophotos, as such coastline vectors were clipped at the mouth of most of the estuaries to avoid confusion with coastal erosion rates.

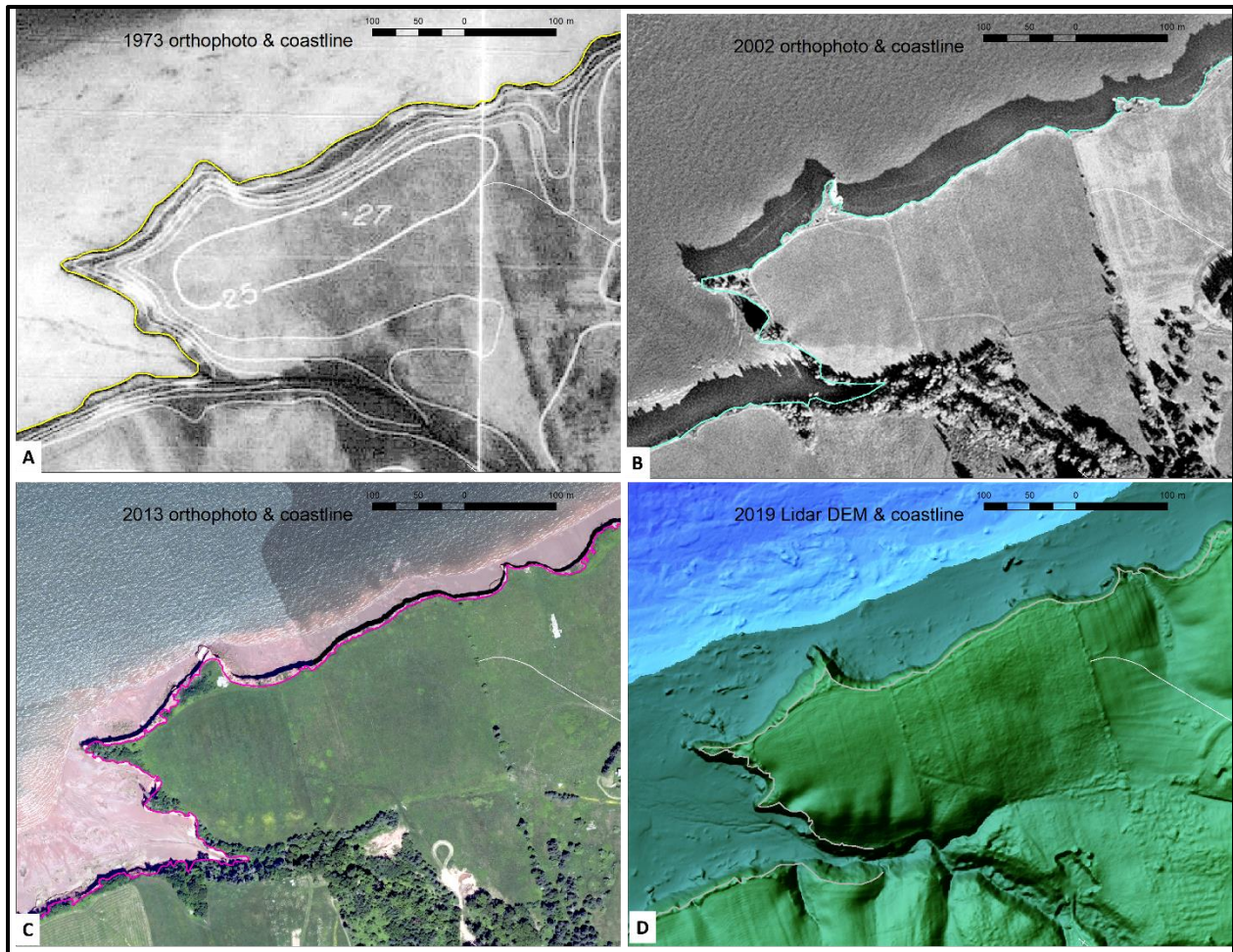


Figure 18. Comparison of orthophotos and coastlines. A) 1973 orthophoto map and coastline (yellow). B) 2002 orthophoto image and coastline (cyan). C) 2013 orthophoto image and coastline (magenta). D) 2019 lidar DEM colour shaded relief image and coastline (grey).

After completing coastline position comparisons between the three dates, it was observed that the 2002 coastline was seaward of the 2013 coastline in many places (Figure 19). This was clearly an error and not a case of accretion (gaining land). Upon closer inspection it appeared that the georeferencing of the 2002 orthophoto was erroneous in places. This made the 2002 coastline unusable for such analysis. It was decided to use the 2019 lidar bare-earth DEM as the most recent coastline feature (Figure 18, Figure 19). A colour shaded relief model of the lidar DEM was constructed to allow for easier interpretation of the top of the bank and coastline. The ability of lidar to “see through” the trees made it ideal for mapping the top of the bank, in fact it was determined to be superior to using the orthophotos since the top of the bank was often obscured by trees and other vegetation in the imagery which also suffered from poor contrast in areas (Figure 18). As a result, the coastlines from 1973, 2012 and 2019 were used for analysis, although some discrepancies with the coastline position remained (Figure 19). These discrepancies were attributed to difficulties in interpreting the coastline from the 1973 orthophoto map.

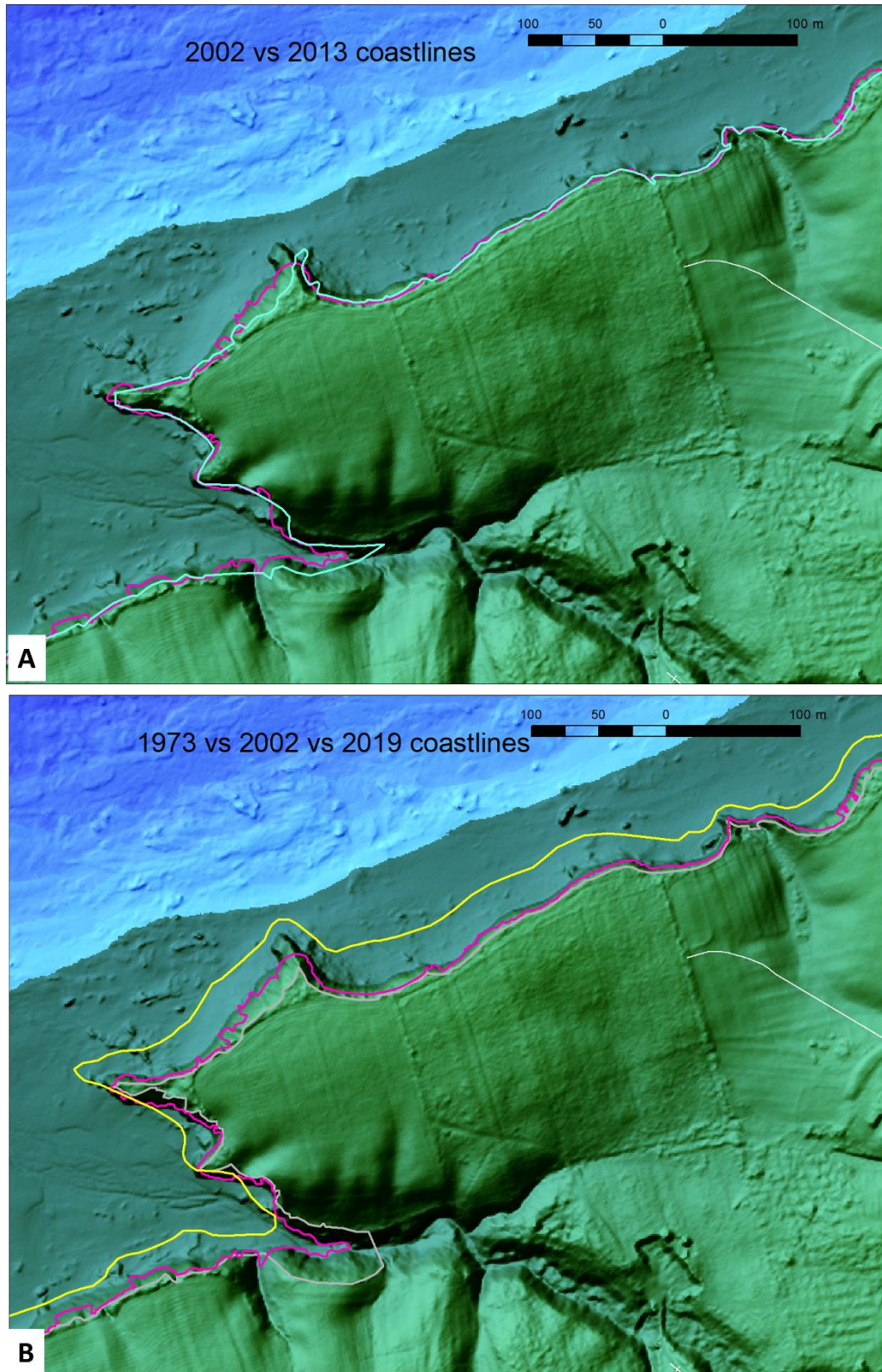


Figure 19. Comparison of coastline positions from historical imagery/lidar. A) Coastlines derived from 2002 (cyan) and 2013 (magenta). B) Coastlines derived from 1973 (yellow), 2013 (magenta) and 2019 lidar DEM (grey).

From this point we conducted GIS analysis to determine the shortest distance between the 2019 coastline and that of the 1973 and 2012 coastline. Here we defined the distance and rate (distance between coastlines divided by the number of years separating the observation) as Long Term (LT) for the 2019 to 1973 distance and erosion rate and Short Term (ST) for the 2019 to 2013 distance and erosion rate. Since this coastal area of Nova Scotia was known for erosion and very little to no accretion, we only considered the rates of erosion, which in our case were denoted by negative values. We calculated the statistics of the LT and ST erosions rates (Figure 20). The LT statistics between the 1973 and 2019 coastlines indicated an average erosion rate of 83 cm/year with a standard deviation of 76 cm/year. The ST statistics between the 2013 and 2019 coastlines indicate an average erosion rate of 190 cm/year with a standard deviation of 225 cm/year. Previous studies of erosion rates in the Maritimes show averages on the order of 20-40 cm/year (Webster, 2012). Although the 1973 coastline is quite generalized and not as detailed at the 2013 or 2019 coastline, the longer time gaps between coastlines (46 years) allowed any errors in the coastline position between the dates to be dampened and their effect lessened because of the large time gap when the rate was calculated (distance/time gap). In the case of the 2013 to 2019 coastlines, the time gap was only 6 years and thus any errors in coastline position are amplified when the rate was calculated.

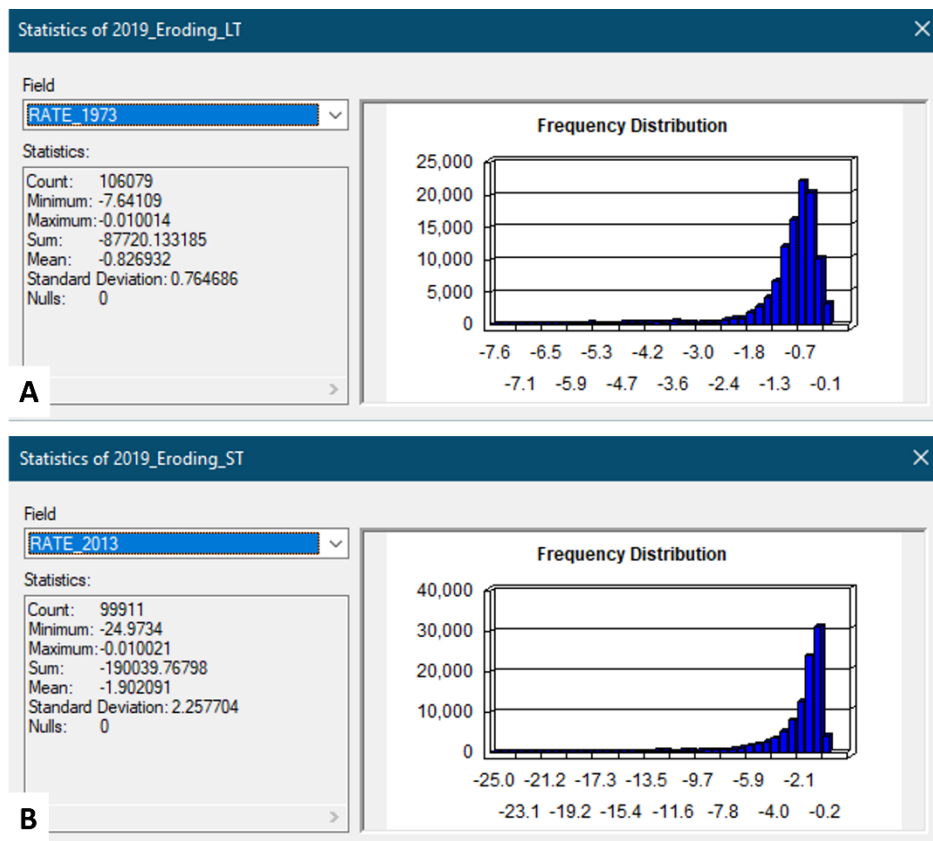


Figure 20. Comparison of LT and ST erosion rates. A) Erosion rate LT statistics between the 1973 and 2019 coastlines. Average rate of 83 cm/year with a standard deviation of 76 cm/year. B) Erosion rate ST statistics between the 2013 and 2019 coastlines. Average rate of 190 cm/year with a standard deviation of 225 cm/year.

Another issue that may have affected the results and calculated rate of erosion was the difference in products used to generate coastline positions. The coastline from the 2013 orthophoto may have been drawn incorrectly where the top of the bank was often obscured by vegetation and where the imagery itself may have contained relief displacement errors. These errors did not exist in the same areas where the 2019 bare earth lidar DEM was used to generate the coastline position. Thus, we are not comparing two similar datasets, but rather one that more clearly shows the top of bank with one that is more uncertain. As a result of these differences and the fact the ST (2013-2019) erosion rate was calculated to be over 2-times that of the LT (1973-2019) erosion rate only the LT rate was used to calculate the projected coastline positions for 2050 and 2100. We caution the users of these data that the erosion rates have a higher degree of uncertainty because of the challenges encountered. We recommend the projected coastlines be used as a warning or a guideline to landowners and not used to implement strict land use policies based on these results. Ideally the province will acquire new lidar at some point in the future to support more robust analysis. We would recommend that a colour shade relief map be constructed from the new lidar and used to interpret the coastline to support comparison with the 2019 position for a more representative calculation of erosion rate. While historical aerial photos can show some changes, the photos can be inaccurate, and the resolution can be poor. As well, RGB photography cannot penetrate vegetation, so the coastline can be obscured. Since lidar can penetrate vegetation, it gives the most accurate representation of the coastline. As well, remote sensing techniques will be able to provide high resolution spatial data on salt marshes (Fagherazzi et al. 2020), which greatly impact coastal erosion. In future data collection, lidar should be used, when possible, to record the coastline.

During the analysis, it was discovered that rivers and waterways needed to be removed from the coastline for the erosion calculation. In the 2013 orthomosaic, several waterways were too obscured by trees to be delineated (Figure 21 and Figure 22). The same waterways were clearly defined in the 2019 lidar data, as the lidar penetrated the trees. Since it was not possible to accurately delineate the coastline for some waterways in multiple datasets, they were omitted from the erosion calculation. Because of this omission, there was no data for the coastline along the mouths of several waterways, which could contribute to errors in the erosion calculation. Therefore, the calculated erosion at the mouths of waterways may not be accurate.

Coastal Vulnerability and Projected Erosion in East Hants County

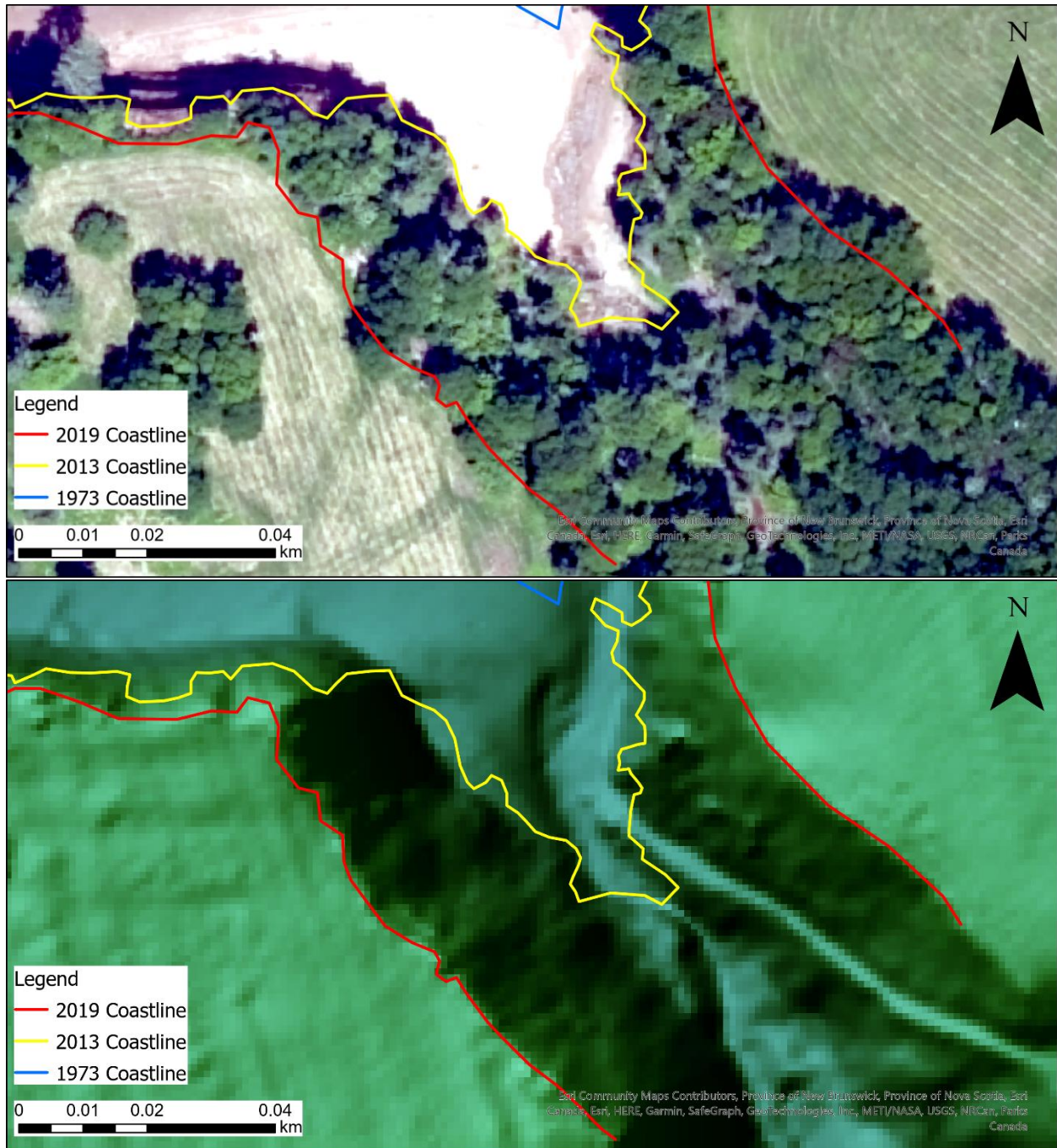


Figure 21. Trees that obscure the 2013 coastline are removed in the 2019 lidar, causing potential error in the distance between the 2013 and 2019 coastlines.

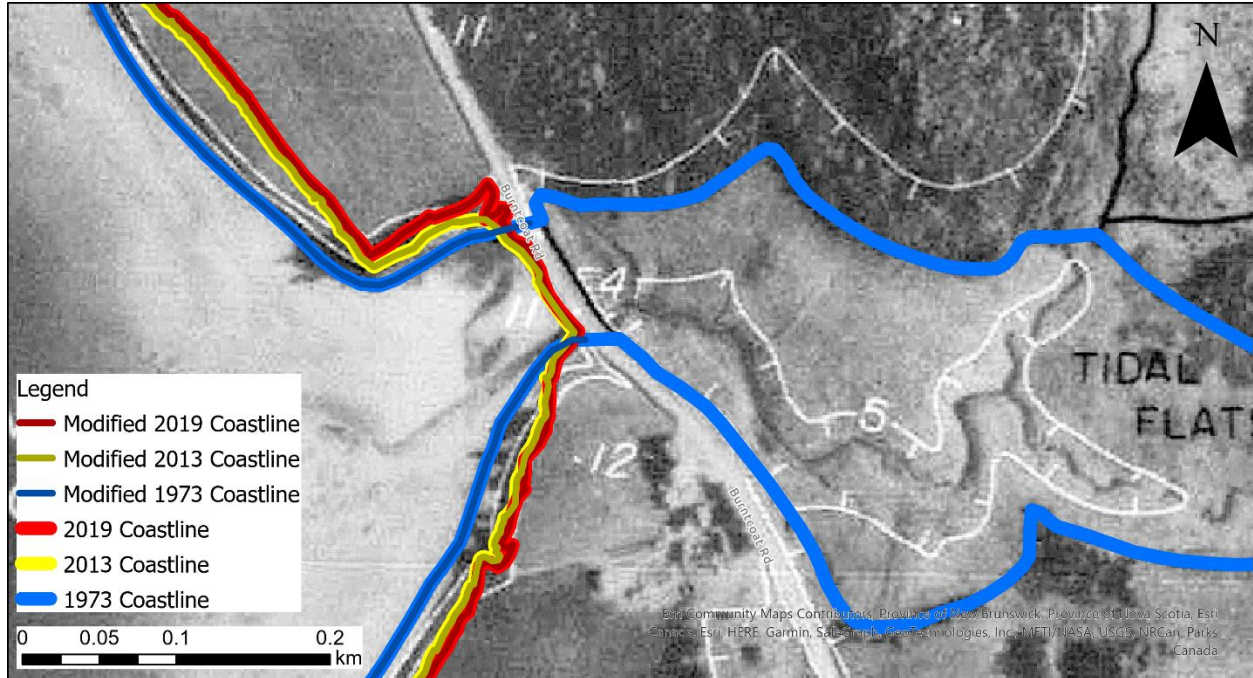


Figure 22. Modified coastlines where the 1973 tidal flat has been omitted from the erosion calculation.

Salt marshes were a possible source of error in the erosion calculations done for this project. The 1973 aerial photos had several present-day salt marshes landward of the coastline that had been manually drawn. Salt marshes in the 2013 photos and 2019 lidar were seaward of the coastline, as they experience tidal action. Because of this difference, there were large distances between the 1973 and 2013 coastline along salt marshes (Figure 23). The erosion rate along salt marsh borders should be considered general and potentially overestimated. While the current rate of erosion along salt marshes may be overestimated, sea-level rise may severely impact erosion in these areas if salt marshes are uprooted or decimated.

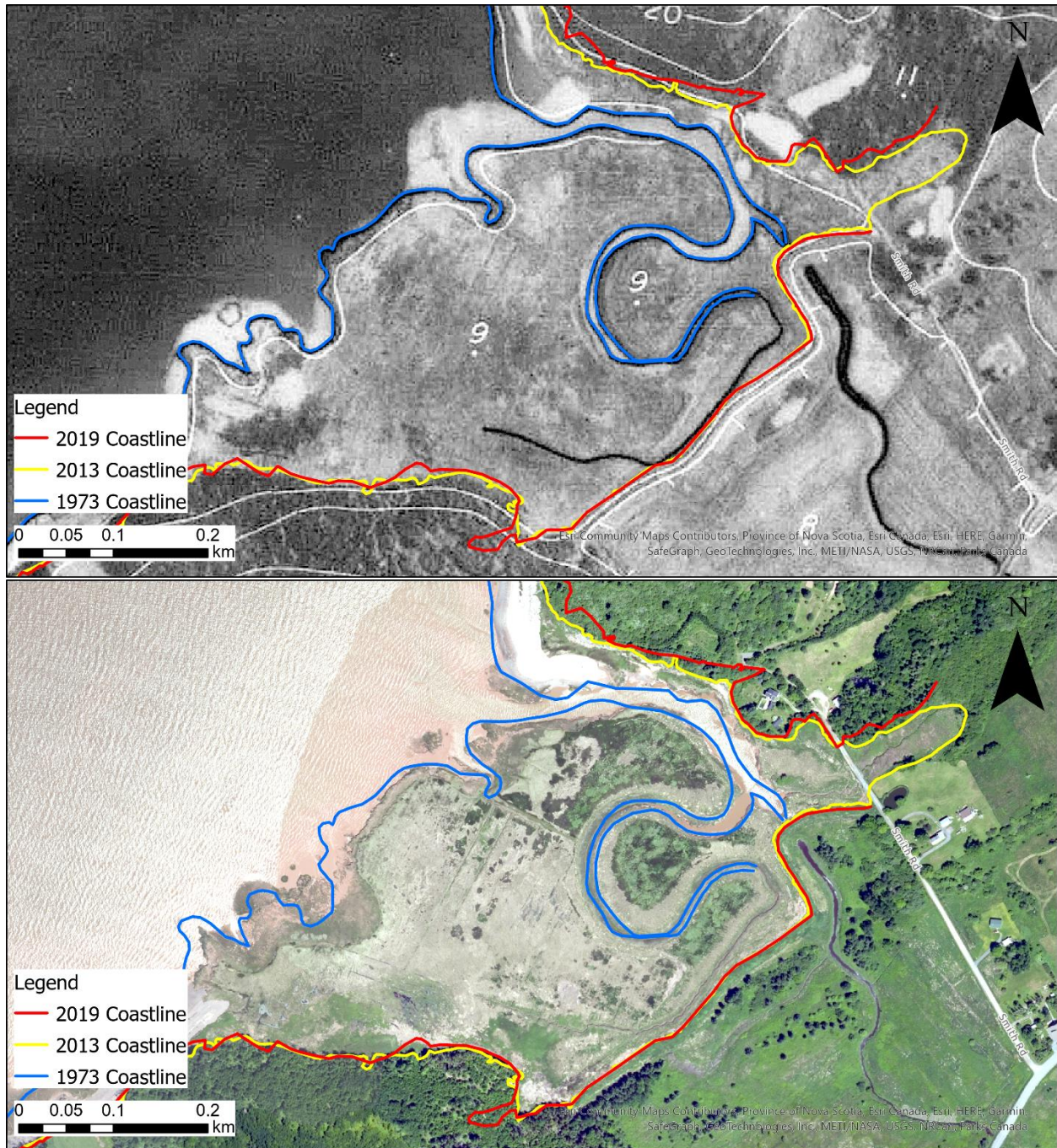


Figure 23. Digitized coastlines along a waterway in 1973 and a salt marsh in 2013.

Dykes presented a challenge to the erosion calculations. In areas where dykes were present, the rate of erosion was expected to be minimal due to the persistence of the dyke armoring. The projected 2100 coastline does not take into consideration coastline repairs or artificial accretion and erosion of coastline along dykes may be overestimated. While it may not be an accurate representation of the erosion while dykes are being maintained, it highlights how serious erosion could be in these areas were the dykes to be damaged or removed.

Coastal Vulnerability and Projected Erosion in East Hants County

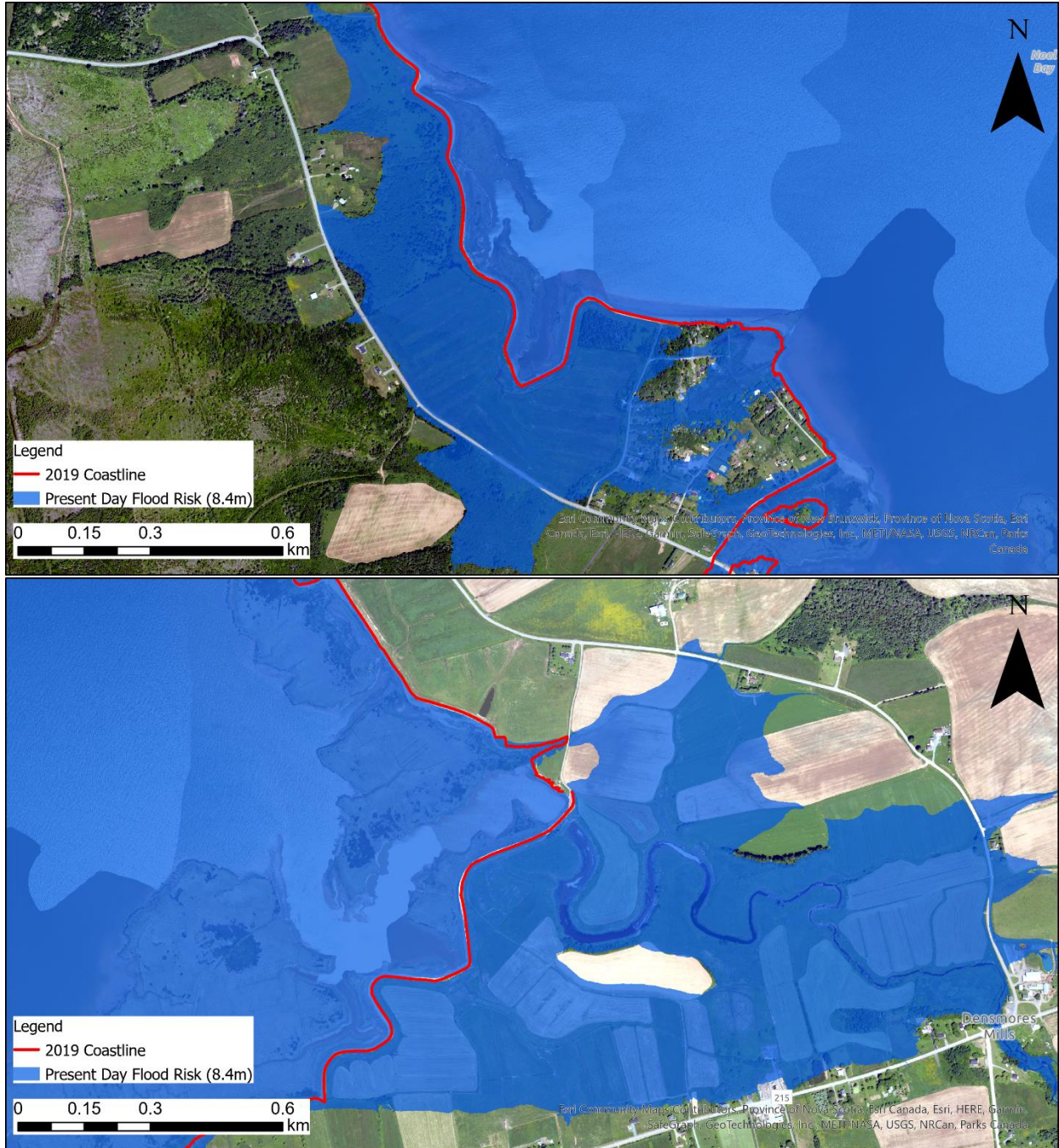


Figure 25. Dykes near Burntcoat (top) and Noel Shore (bottom) under present day flood risk conditions.

6. References

- Bernier, N.B. (2005) Annual and seasonal extreme sea levels in the Northwest Atlantic: hindcasts over the last 40 years and projections for the next century. PhD thesis, Dalhousie University.
- Bernier, N.B., Thompson, K.R. (2006) Predicting the frequency of storm surges and extreme sea levels in the Northwest Atlantic. *J Geophys Res* 111:10009. doi:10.1029/2005JC003168.
- Cheng, L., Abraham, J., Hausfather, Z., & Trenberth, K. E. (2019). How fast are the oceans warming? *Science*, 363(6423), 128–129.
- Church, J.A., P.U. Clark, A. Cazenave, J.M. Gregory, S. Jevrejeva, A. Levermann, M.A. Merrifield, G.A. Milne, R.S. Nerem, P.D. Nunn, A.J. Payne, W.T. Pfeffer, D. Stammer and A.S. Unnikrishnan, 2013a. Sea Level Change. In: *Climate Change 2013: The Physical Science Basis. Contribution of Working Group I to the Fifth Assessment Report of the Intergovernmental Panel on Climate Change* [Stocker, T.F., D. Qin, G.-K. Plattner, M. Tignor, S.K. Allen, J. Boschung, A. Nauels, Y. Xia, V. Bex and P.M. Midgley (eds.)]. Cambridge University Press, Cambridge, United Kingdom and New York, NY, USA.
- Church, J.A., P.U. Clark, A. Cazenave, J.M. Gregory, S. Jevrejeva, A. Levermann, M.A. Merrifield, G.A. Milne, R.S. Nerem, P.D. Nunn, A.J. Payne, W.T. Pfeffer, D. Stammer and A.S. Unnikrishnan, 2013b. Sea Level Change Supplementary Material. In: *Climate Change 2013: The Physical Science Basis. Contribution of Working Group I to the Fifth Assessment Report of the Intergovernmental Panel on Climate Change* [Stocker, T.F., D. Qin, G.-K. Plattner, M. Tignor, S.K. Allen, J. Boschung, A. Nauels, Y. Xia, V. Bex and P.M. Midgley (eds.)].
- Daigle, R. and Project Research Team. 2006. Impacts of sea level rise and climate change on the coastal zone of southeastern New Brunswick/ Impacts de l'élévation du niveau de la mer et du changement climatique sur la zone côtière du sud-est du Nouveau-Brunswick. Environment Canada, 611 pp. (also on CD-ROM and on-line at <http://atlantic-web1.ns.ec.gc.ca/slr/>).
- Daigle, R.J. 2016. Sea-Level Rise and Coastal Flooding Estimates for Hantsport.
- Daigle, R.J. 2017. Sea-Level Rise and Flooding Estimates for New Brunswick Coastal Sections 2017
- Fagherazzi, S., Mariotti, G., Leonardi, N., Canestrelli, A., Nardin, W., & Kearney, W. S. (2020). Salt marsh dynamics in a period of accelerated sea level rise. *Journal of Geophysical Research: Earth Surface*, 125(8).
- Fisheries and Oceans Canada. (2014). Canadian Extreme Water Level Adaptation Tool Website. Retrieved 25 March 2017 from Fisheries and Oceans Canada.
- FitzGerald, D. M., & Hughes, Z. (2019). Marsh processes and their response to climate change and sea-level rise. *Annual Review of Earth and Planetary Sciences*, 47, 481-517.
- Golledge, N. R. (2020). Long-term projections of sea-level rise from ice sheets. *Wiley Interdisciplinary Reviews: Climate Change*, 11(2), e634.
- Han G., Z. Ma, L. Zhai, B. Greenan and R. Thomson 2016. Twenty-first century mean sea level rise scenarios for Canada. Canadian Technical Report. Hydrography and Ocean Science. Fisheries and Oceans Canada. 313: x + 19 pp.
- IPCC, 2014: *Climate Change 2014: Synthesis Report. Contribution of Working Groups I, II and III to the Fifth Assessment Report of the Intergovernmental Panel on Climate Change* [Core Writing Team, R.K. Pachauri and L.A. Meyer (eds.)]. IPCC, Geneva, Switzerland, 151 pp.

Coastal Vulnerability and Projected Erosion in East Hants County

- IPCC 4th Assessment Report, Climate change 2007: The physical Science Basis. Contribution of Working Group I to the Fourth Assessment report of the Intergovernmental Panel on Climate Change [Solomon S., D. Qin, M. Manning, Z. Chen, M. Marquis, K.B. Averyt, M. Tignor and H.L. Miller (eds.)]. Cambridge University Press, Cambridge, UK, and New York, USA., 2007.
- James, T.S., Henton, J.A., Leonard, L.J., Darlington, A., Forbes, D.L., and Craymer, M., 2014. Relative Sea-level Projections in Canada and the Adjacent Mainland United States; Geological Survey of Canada, Open File 7737, 72 p.
- Jamieson, R., Kurylyk, B., Rapaport, E., Manuel, P., Van Proosdij, D., Beltrami, H., Hayward, J., KarisAllen, J., Clark, K., Tusz, C., Jahncke, R., García-García, A., & Cuesta-Valero, F.,J. (2019). Standard for the incorporation of climate change into riverine and coastal flood mapping in Nova Scotia. Technical report prepared for the Government of Nova Scotia. Halifax, Nova Scotia, 196 pp.
- Parris, A., P. Bromirski, V. Burkett, D. Cayan, M. Culver, J. Hall, R. Horton, K. Knuuti, R. Moss, J. Obeysekera, A. Sallenger, and J. Weiss, 2012. Global sea level rise scenarios for the US National Climate Assessment. NOAA Tech Memo OAR CPO-1. 37 pp.
- Richards and Daigle (2011) Scenarios and Guidance for Adaptation to Climate Change and Sea-Level Rise – Nova Scotia and Prince Edward Island Municipalities.
- van Proosdij, D., Ross, C., & Matheson, G. (2018). Risk Proofing Nova Scotia Agriculture: Nova Scotia Dyke Vulnerability Assessment. Saint Mary's University: Halifax, NS, Canada, 51.
- van Proosdij, D., Jahncke, R. 2019. Nova Scotia Floodline Delineation: Guidance for Sea Level Rise and Storm Surge Projections. NS department of Municipal Affairs.
- Webster, T, McGuigan, K., MacDonald, C. 2012. Lidar processing and Flood Risk Mapping for the Communities of the District of Lunenburg, Oxford-Port Howe, Town and District of Yarmouth, Chignecto Isthmus and Minas Basin. Atlantic Climate Adaptation Solutions (ACAS), Nova Scotia Coastal Flood Risk Mapping Program. Available at http://atlanticadaptation.ca/sites/discoveryspace.upei.ca/acasa/files/Flood%20risk%20in%20ACAS%20municipalities_0_0.pdf
- Webster, T. and Stiff, D. (2008). The prediction and mapping of coastal flood risk associated with storm surge events and long-term sea level changes. In Risk Analysis VI Simulations and Hazard Mitigation. WIT Press. Edited by Brebbia, C.A. and Beriatos, E. pp. 129-139.
- Zhai L., B. Greenan, J. Hunter, T.S. James, G. Han, R. Thomson, and P. MacAulay 2014. Estimating Sea-level Allowances for the coasts of Canada and the adjacent United States using the Fifth Assessment Report of the IPCC. Canadian Technical Report. Hydrography and Ocean Science. Fisheries and Oceans Canada. 300: v + 146 pp.
- Zhai, L., Greenan, B., Hunter, J., James, T., Han, G., MacAulay, P. & Henton, J. 2015. Estimating Sea-Level Allowances for Atlantic Canada using the Fifth Assessment Report of the IPCC, Atmosphere-Ocean, 53:5, 476-490, DOI: 10.1080/07055900.2015.1106401.